Stratospheric influence on marine cold air outbreaks in the Barents Sea

Hilla Afargan-Gerstman[1], Iuliia Polkova[2], Lukas Papritz[1], Paolo Ruggieri[3,4], Martin P. King[5], Panos J. Athanasiadis[4], Johanna Baehr[2], and Daniela I.V. Domeisen[1]

[1]Institute for Atmospheric and Climate Science, ETH Zürich, Zürich, Switzerland
[2]Institute of Oceanography, Universität Hamburg, CEN, Hamburg, Germany
[3]Department of Physics and Astronomy, University of Bologna, Italy
[4]Euro-Mediterranean Center on Climate Change (CMCC), Bologna, Italy
[5]NORCE Climate, and Bjerknes Centre for Climate Research, Bergen, Norway

Correspondence: Hilla Afargan-Gerstman (hilla.gerstman@env.ethz.ch)

Abstract. Marine cold air outbreaks (MCAOs) in the Arctic are associated with a range of severe weather phenomena, such as polar lows, strong surface winds and intense cooling of the ocean surface. While MCAO frequency has been linked to the strength of the stratospheric polar vortex, a connection to the occurrence of extreme stratospheric events, known as sudden stratospheric warmings (SSWs), has dominantly been investigated with respect to cold extremes over land. Here, the influence of SSW events on MCAOs in the Barents Sea is studied using observational and reanalysis datasets. Overall, more than a half of SSW events lead to more frequent MCAOs in the Barents Sea. SSW events with an enhanced MCAO response in the Barents Sea are associated with a ridge over Greenland and a trough over Scandinavia, leading to an anomalous dipole pattern of 500-hPa geopotential height and strong northerly flow over the Norwegian Sea. As SSW events tend to have a long-term influence on surface weather, these results can shed light on the predictability of MCAOs in the Arctic for winters with SSW events.

1 Introduction

Marine cold air outbreaks (MCAOs) in the Arctic are characterized by large-scale advection of cold polar air masses over open ocean. These events are associated with a range of severe weather phenomena, such as polar lows (e.g., Mansfield, 1974; Rasmussen et al., 2004; Kolstad, 2011; Mallet et al., 2013; Radovan et al., 2019), strong surface winds (Kolstad, 2017), and intense ocean-atmosphere heat exchange, playing an important role for deep-water formation (e.g., Isachsen et al., 2013; Buckley and Marshall, 2016).

The occurrence of MCAOs over the Norwegian Sea and the Barents Sea has been associated with Arctic air masses carried by northerly or easterly winds (Kolstad et al., 2009; Papritz and Spengler, 2017). These winds are in near-geostrophic balance and, in particular, northerly winds are associated with a regional pressure dipole pattern (Kolstad et al., 2009; Jahnke-Bornemann and Brümmer, 2009), consisting of a high pressure anomaly near Iceland or Greenland and a low pressure anomaly over Scandinavia and towards Svalbard. Systematically linking large-scale flow variability and MCAO occurrence revealed that

particularly favorable conditions for MCAO formation in the northeastern North Atlantic occur during cyclonically dominated weather regimes, such as the Scandinavian trough and Atlantic ridge regimes (Papritz and Grams, 2018). In contrast, blocked regimes with anticyclonic anomalies over northern Europe (such as European or Scandinavian blocking) tend to suppress
25   MCAO occurrence, with the exception of Greenland blocking. The link between large-scale flow regimes and the frequency of MCAOs in the Nordic Seas is suggested to arise from shifts in the strength and the location of cyclone activity (Papritz and Grams, 2018). In particular, periods of intense storm track activity associated with cyclonic weather regimes are found to be favorable for MCAOs.

The stratosphere can have a significant impact on surface weather in the North Atlantic and Europe. This has dominantly
30   been investigated with respect to cold temperature extremes over land, where cold air outbreak frequency has been linked to the strength of the stratospheric polar vortex (Thompson et al., 2002; Kolstad et al., 2010). Extreme changes in the strength of the stratospheric polar vortex, such as sudden stratospheric warming (SSW) events, favour changes in weather patterns over Europe, often leading to a negative signature of the North Atlantic Oscillation (NAO; e.g., Baldwin and Dunkerton, 2001; Limpasuvan et al., 2004; Butler et al., 2017; Domeisen, 2019), though with large tropospheric differences between events
35   (Domeisen et al., 2020). These anomalies can persist for up to 2 months, thus providing a key for a better predictive skill of surface weather on sub-seasonal to seasonal time scales (Sigmond et al., 2013; Scaife et al., 2016; Domeisen et al., 2019). Over Europe, weak vortex events are associated with up to 50% more cold days compared to climatology (Kolstad et al., 2010), while about 60% of the observed cold temperature extremes in midlatitude Eurasia since 1990 can be explained by weak stratospheric polar vortex states (Kretschmer et al., 2018).

40   Since the previously discussed dominant pressure dipole pattern favouring MCAOs over the Nordic Seas is relatively independent of the NAO (e.g., Jahnke-Bornemann and Brümmer, 2009), the question arises to what extent the modulation of North Atlantic surface weather by stratospheric variability affects MCAO frequency. While the frequency of cold extremes over land has been shown to increase in response to weak stratospheric forcing, Papritz and Grams (2018) found indications that for winters with a weak stratospheric polar vortex, MCAOs are in fact less frequent in certain regions, namely the Greenland
45   and Iceland Seas due to a weakening of the storm track in the Norwegian Sea, whereas in the Barents Sea a modest increase of MCAO frequency was found. This suggests a spatially complex, not yet fully understood linkage between stratospheric variability and MCAO formation.

Here, the role of stratospheric extreme events in setting favorable conditions for MCAO occurrence over the North Atlantic is revisited using atmospheric reanalysis. Particularly, we focus on the Norwegian and Barents Seas where the occurrence of
50   polar lows is frequent and poses a risk on the increasing human activity and along the fairly densely populated Norwegian coast. Enhanced predictability of MCAOs in these regions would therefore be societally and economically beneficial. In addition, the Barents Sea is the region with the most dramatic changes associated with Arctic amplification (Cohen et al., 2014). Our results aim to shed light on the predictability of MCAOs over the Barents and Norwegian Seas, and contribute to the understanding of MCAO occurrence in these regions.

2 Data and Methodology

2.1 Data

We use daily reanalysis data from the European Centre for Medium-Range Weather Forecasts (ECMWF) ERA-Interim dataset (Dee et al., 2011) for the years 1979 to 2016. A climatology is defined using daily averages for this period (1979–2016), and daily anomalies are computed as deviations from the climatology.

To characterize storm track activity in the large-scale flow, we use cyclone frequencies derived from sea level pressure with the method by Wernli and Schwierz (2006). A similar approach has been implemented in Papritz and Grams (2018).

2.2 MCAO index definition

We use the MCAO index (M) for the classification of marine cold air outbreaks. The MCAO index was designed to detect the flow of cold air over a warmer ocean (Kolstad and Bracegirdle, 2008; Papritz et al., 2015; Polkova et al., 2019) and is defined as

$$\mathrm{M} = \theta_{\mathrm{skt}} - \theta_{\mathrm{850hPa}} \tag{1}$$

where θ_{skt} is the potential temperature at the ocean surface, computed from skin temperature and surface pressure. θ_{850hPa} is the potential temperature at 850 hPa. The MCAO index is defined only over the ocean, thus land grid points are masked. Only positive potential temperature differences ($\theta_{skt} - \theta_{850hPa} > 0$ K), which indicate a state of atmospheric instability associated with upward sensible heat fluxes, are considered. Values of the MCAO index (Eq. 1) that exceed a threshold of 4K are categorized as moderate-to-intense MCAOs (e.g., Papritz and Spengler, 2017).

2.3 Characterization of the large-scale flow

We define a new index based on the 500-hPa geopotential height anomaly from climatology (Z'). The index, named the Zonal Dipole Index (ZDI), equals to half of the difference in Z' between the spatial average over two main areas that modulate the frequency of MCAOs in the Norwegian Seas and the Barents Sea (enclosed by the grey boxes in Fig. 3b): southeast of Greenland (Z'_G, 30°W-50°W, 60°N-70°N) and northern Europe (Z'_E, 30°E-50°E, 60°N-70°N), as follows

$$\mathrm{ZDI} = \frac{Z'_{\mathrm{G}} - Z'_{\mathrm{E}}}{2}. \tag{2}$$

Note that in contrast to weather regimes that are identified by cluster analysis (e.g., Papritz and Grams, 2018; Beerli and Grams, 2019), a given value of the ZDI index may correspond to more than one weather regime.

2.4 SSW events

Extreme changes in the stratospheric polar vortex can affect surface weather in the North Atlantic and Europe (e.g., Baldwin and Dunkerton, 2001; Limpasuvan et al., 2004; Butler et al., 2017). To assess the impact of the stratosphere on MCAO occur-

rence, we examine the changes in the MCAO frequency in response to 24 historical major SSW events between 1979–2016. Major SSWs occur when the westerlies associated with the winter stratospheric polar vortex reversal to easterlies. A common definition for major SSWs is the central date for which the daily mean zonal-mean zonal winds at 10 hPa and 60°N first change from westerly to easterly between November and March (Charlton and Polvani, 2007). For a list of major SSW events in the ERA-Interim reanalysis, see Butler et al. (2017).

The MCAO response to SSW events is here defined as the change in MCAO frequency or index over a period of 30 days after the onset of the SSW (i.e., the SSW central date). The MCAO frequency is computed for MCAOs with a magnitude above a 4K threshold.

3   Results

3.1   Stratospheric influence on MCAO occurrence following SSW events

Fig. 1a demonstrates the regional distribution of the 90th percentile of the climatological MCAO index, averaged from December to March (DJFM). The MCAO index is strongest over three main regions: the Labrador Sea (and south of Greenland), the Norwegian Sea and the Barents Sea (black boxes in Fig. 1a). MCAOs are also most frequent over these regions (Fig. 1b), with a likelihood of more than 40% for an occurrence of moderate-to-extreme MCAOs in the Labrador Sea during DJFM, and nearly 35% in the Norwegian Sea and the Barents Sea.

We examine the changes in the MCAO index in response to major SSW events in the reanalysis. Major SSW events tend to be followed by anomalously cold temperatures over the western North Atlantic and Eurasia (Fig. 1c). When all major SSW events between 1979–2016 (Table 1) are considered, the MCAO response to SSW events exhibits significant regional variability, with the largest increase of MCAO frequency over the western Barents and Norwegian Seas and a decrease along the sea ice edge over the Greenland Sea as well as the Labrador Sea (Fig. 1d).

In addition to the regional variability of the MCAO response, there is a wide variability among the SSW events. To assess this variability, we analyze the changes in the MCAO frequency over a period of 30 days after the onset of a SSW. We focus on the Barents Sea (70°N to 78.5°N, 30°E to 50°E, easternmost box in Fig. 1a). More than a half of the SSW events between 1979–2016 are followed by a change in the MCAO frequency that is equal to or above the mean MCAO frequency in DJFM (i.e., frequency of about 23%, Fig. 2). We classify the upper tercile of SSW events as having a strong Barents Sea response (12/1981, 01/1985, 01/1987, 12/1987, 12/2001, 01/2003, 02/2010 and 01/2013). These events are followed by MCAO frequencies that exceed 30% for a period of 30 days (Fig. 2). Using this classification, we are able to capture the favorable conditions for MCAO occurrence in response to stratospheric forcing. The classified SSW events are highlighted in bold in Table 1.

Fig. 3a demonstrates the anomalies of the MCAO index following these SSW events, showing an increased MCAO magnitude over the Norwegian and the Barents Seas, and a decrease over the Labrador Sea. Note that the change in MCAO index magnitude is consistent with the MCAO frequency anomalies for these SSWs. In the next section, we aim to link these anomalies to the influence of the stratosphere on the large-scale atmospheric circulation.
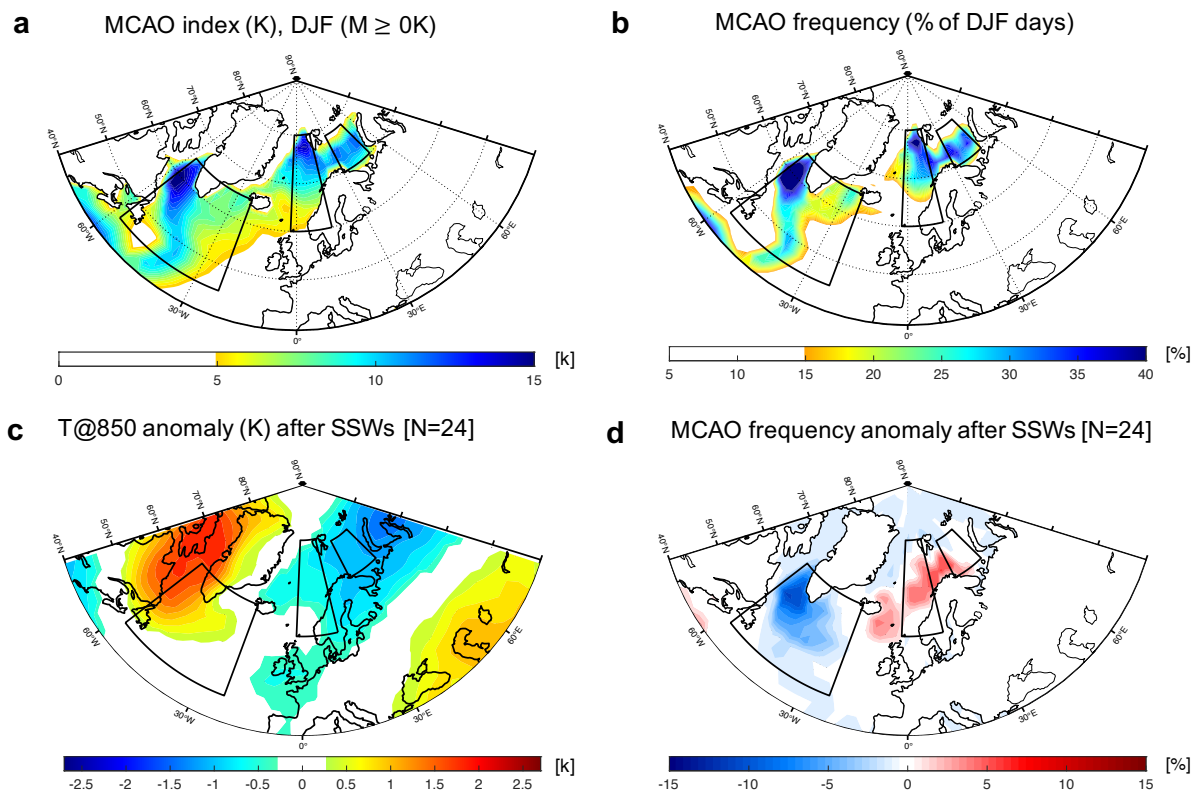
Figure 1. (a) The 90th percentile of the MCAO index (color shading, in K) and (b) the MCAO frequency (shading, indicated by the percentage of days for which the MCAO index exceeds 4K) in the DJFM climatology based on ERA-Interim reanalysis. (c) The average 850-hPa temperature anomaly (shading, in K) and (d) the MCAO frequency anomaly (shading in percentage of days out of a 30-day period) over a period of 30 days following 24 historical SSW events. Black boxes show the three regions of interest: the Labrador Sea (and south of Greenland), the Norwegian Sea and the Barents Sea, where the climatological MCAO index is highest. Only statistically significant values above the 95% level are shown (based on a two-sided Student's *t test)*.

3.2 Connection to large-scale atmospheric circulation patterns

To examine how stratospheric variability contributes to the anomalous occurrence of MCAOs in the Barents Sea, we analyse the regional tropospheric patterns following the SSWs with enhanced Barents Sea MCAOs. We focus on a period of 30 days after the onset of the SSWs. Fig. 3b shows a composite of the 500-hPa geopotential height and wind anomalies relative to the SSW central dates. Following SSWs with a strong Barents Sea response, positive geopotential height anomalies centred over the south-eastern part of Greenland and negative anomalies over northwest Eurasia are found. This pattern corresponds to anomalous northerly winds over the Norwegian Sea (Fig. 3c), resulting in a southward advection of Arctic air masses.

Thus, we find that SSW events with enhanced MCAOs in the Barents Sea are accompanied by: (i) a strong high-pressure anomaly over south-eastern Greenland ("Greenland Blocking"), (ii) a low-pressure anomaly over Scandinavia ("Scandinavian
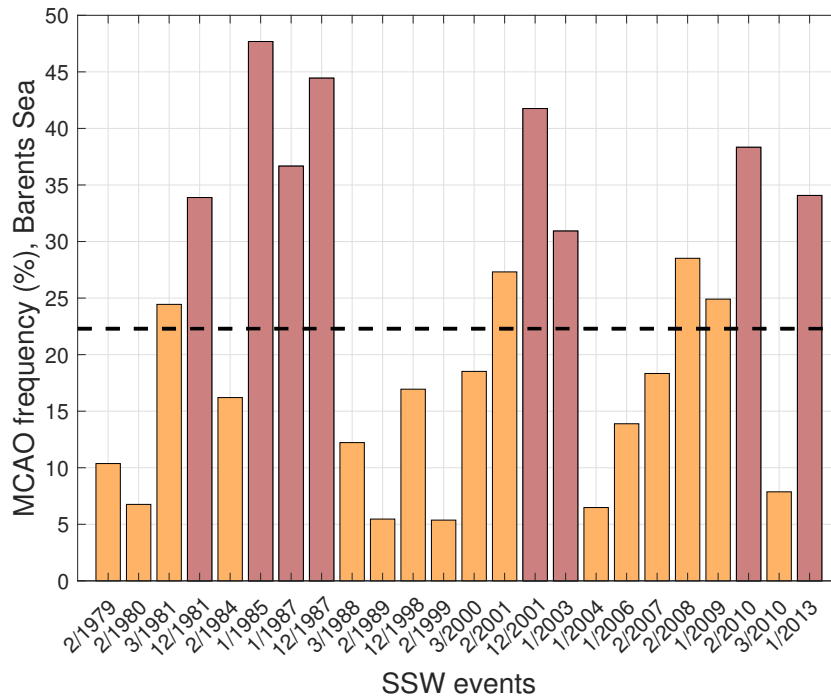
Figure 2. MCAO frequency (%) averaged over the Barents Sea region (see box dimensions in Fig. 1a) following 24 historical SSW events. For each SSW event, we analyze the number of days for which M≥4K for a period of 30 days following the onset of the SSW event. SSW events with an enhanced MCAO response in the Barents Sea are indicated by a darker shading. The solid black line represents the mean MCAO frequency over the Barents Sea based on the DJFM climatology.

Trough"), and (iii) strong northerly winds across the Norwegian Sea (Fig. 3b,c). Note that (iii) is strongly constrained by (i) and

125 (ii). These patterns are associated with a southward shift of the storm track over the North Atlantic, consistent with the large-scale anomalous patterns following SSW events which are often associated with a negative phase of the NAO (e.g., Kidston et al., 2015; Afargan-Gerstman and Domeisen, 2020). Furthermore, a strong reduction in cyclone frequency is observed in the Norwegian Seas, leading to a reduced MCAO frequency along the sea ice edge in the Greenland Sea. At the same time, cyclone frequency is strongly increased over Scandinavia and in the eastern Barents Sea, which provides favourable conditions

130 for MCAOs there.

To evaluate the link between MCAOs and the spatial structure of the geopotential height anomaly, we compute the relation between the ZDI, defined in Eq. 2, and the MCAO index over the Barents Sea in the winter climatology. We use an extended winter period between December and March (DJFM) since the 30-day SSW response may extend into March. The dependence between these indices is shown by a linear regression, as follows

135 $$M = b_M \cdot ZDI, \tag{3}$$
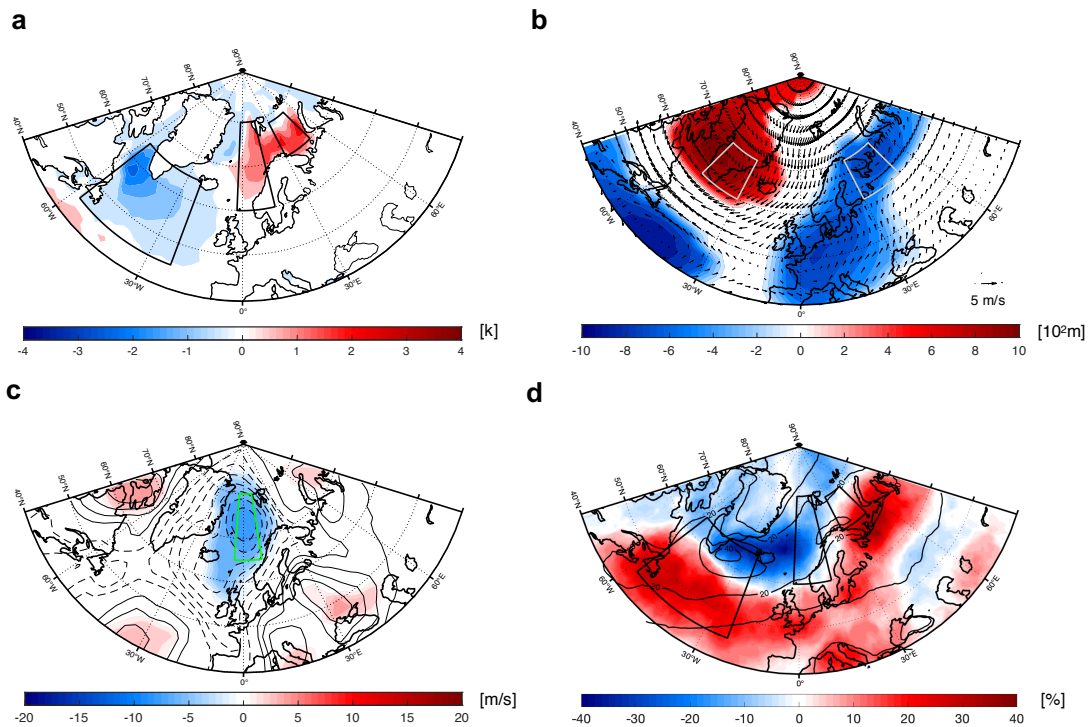
Figure 3. Regional flow patterns following SSW events with enhanced MCAO response in the Barents Sea. (a) MCAO index anomaly (color shading, in K) after SSW events with a strong Barents Sea response (8 events), in which the average MCAO frequency exceeds a threshold of 30% over a period of 30 days after the onset on the SSW event (Fig. 2). Composites of (b) geopotential height anomaly at 500 hPa (shading, in 10^2 m), and (c) meridional wind anomaly at 300 hPa (shading, in m s^{-1}) averaged over a period of 30 days after the same SSW events as in (a). Wind anomalies at 300 hPa are indicated in panel (b) (arrows, in m s^{-1}). (d) Cyclone frequency anomaly (shading) over a period of 30 days following the SSWs as in (a). The winter climatology of cyclone frequency is shown by black contours (from 10%, in intervals of 10%). Only statistically significant values above the 95% level are shown (based on a two-sided Student's *t test).*

where M is the MCAO index and b_M is the linear regression coefficient. When SSW events with a strong Barents Sea response are considered (triangles in Fig. 4a), a positive linear relation between the MCAO index and the ZDI index is found. Approximately 44% of the variance can be explained by this relation (R^2=0.44). A positive yet weaker relation is found in climatology (circles, R^2=0.15), suggesting that after SSW events there is a higher correlation between MCAOs in the Barents Sea and the

140 occurrence of a large-scale dipole pattern over this region compared to climatology. Furthermore, in periods which exclude SSW events but have a strong response in the Barents Sea, the correlation between the MCAO index and the ZDI index is weaker than in climatology (R^2=0.11, shown in blue). These periods are defined as weeks which are not within the 30-day periods after SSW events but have a strong MCAO index in the Barents Sea (see section 3.1).

The dependence of the meridional wind speed over the northern Norwegian Sea (5°W–10°E, 65°N–80°N, green box in

145 Fig. 3c) on the MCAO index in the Barents Sea is demonstrated in Fig. 4b. The northern Norwegian Sea region is characterized by strong northerly winds that accompany the pressure dipole pattern. We find that for SSW events with enhanced Barents Sea response there is a negative relationship between the meridional wind anomaly over the Norwegian Sea and the MCAO index over the Barents Sea (Fig. 4b). This relationship is stronger in the aftermath of SSW events (R^2=0.13) compared to periods without SSW events.

150 To better understand the dependency of the dipole index on the Barents Sea MCAO index, we distinguish between geopotential height anomalies that correspond to an enhanced Greenland blocking (GB) and those that correspond to a deeper Scandinavian Trough (ST). These indices correspond to the Z'_G and Z'_E defined in Eq. 2. The linear regression between these indices following SSW events with a strong Barents Sea response indicates a positive correlation between Barents Sea MCAO index and the GB index (Fig. 4c), however with a larger spread compared to the ZDI and northerly wind indices. A negative

155 correlation is found with the ST index, which accounts for approximately 42% of the variance after these SSWs (Fig. 4d). We note that the correlation between the MCAO index and the ST index is lower in periods without SSW events (R^2=0.11), and relative to climatology (R^2=0.14).

Overall, these findings suggest a relation between the ZDI index and the MCAO index in the Barents Sea, linking the large-scale geopotential height anomaly pattern with the formation of MCAOs in this region. After SSW events with an enhanced

160 MCAO response in the Barents Sea, there is a higher correlation between the MCAO index and the ZDI index, relative to periods without the occurrence of such SSW events. A similar correlation is found for the ST index, both in climatology and after SSW events, hinting at the importance of a low pressure anomaly over northern Eurasia as the key ingredient for MCAOs in the Barents Sea.

3.3 Relevance of the geopotential height index for the occurrence of MCAOs

165 In winter, the Euro-Atlantic sector may be dominated by cyclonic and blocked large-scale flow features (e.g., Beerli and Grams, 2019; Papritz and Grams, 2018). In a cyclonic flow pattern, a negative geopotential height anomaly (relative to DJFM climatology) dominates at 500 hPa. These negative anomalies are associated with enhanced cyclonic activity, and correspond to more than one dominant weather regime, such as Atlantic or Scandinavian Troughs (Beerli and Grams, 2019). Positive geopotential height anomalies, on the other hand, are linked to blocked weather regimes, such as Greenland blocking, and

Table 1. List of historical SSW events in ERA-Interim reanalysis (as in Butler et al., 2017) and their corresponding ZDI, Z'_{GB} and Z'_{ST} indices. SSWs followed by enhanced MCAO anomalies (as defined in section 2.2) in the Barents Sea are highlighted in bold.

SSW event date	ZDI	Z'_{GB}	Z'_{ST}
22-Feb-79	1.18	1.13	-1.24
29-Feb-80	0.21	6.73	6.32
4-Mar-81	4.69	1.84	-7.54
4-Dec-81	**6.22**	**12.00**	**-0.37**
24-Feb-84	-2.0	3.7	7.6
1-Jan-85	**9.8**	**12.4**	**-7.2**
23-Jan-87	**11.5**	**11.0**	**-12.0**
8-Dec-87	**7.7**	**3.22**	**-12.2**
14-Mar-88	-1.5	1.4	5.4
21-Feb-89	-8.6	-14.1	3.4
15-Dec-98	0.2	-2.3	-2.6
26-Feb-99	-0.5	6.7	7.7
20-Mar-00	2.8	5.1	-0.6
11-Feb-01	6.8	6.2	-7.5
30-Dec-01	**14.7**	**18.0**	**-11.5**
18-Jan-03	**0.6**	**-1.4**	**-2.8**
5-Jan-04	1.4	7.0	4.2
21-Jan-06	0.9	4.4	2.4
24-Feb-07	0.2	1.2	0.7
22-Feb-08	1.8	-7.8	-11.5
24-Jan-09	-3.5	0.6	7.8
9-Feb-10	**8.3**	**17.5**	**1.0**
24-Mar-10	0.4	4.3	3.5
6-Jan-13	**0.4**	**-1.0**	**-1.93**
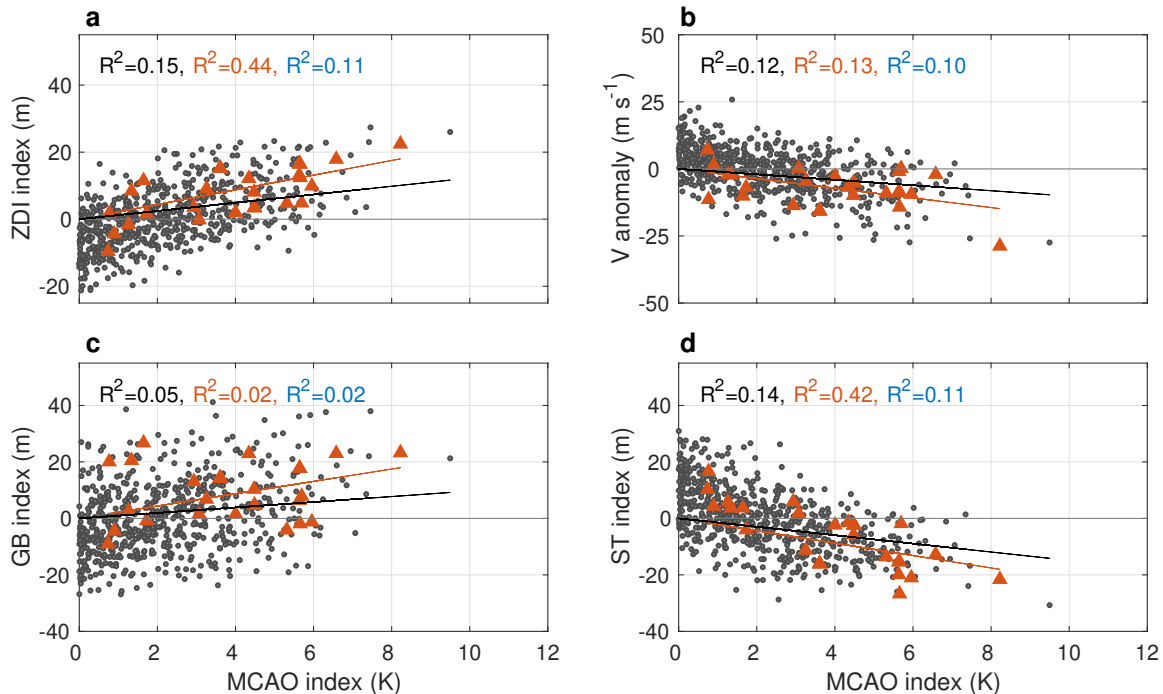
Figure 4. The relation between (a) the weekly averaged ZDI index (circles) and the weekly MCAO index (M) over the Barents Sea during DJFM in reanalysis. Linear regressions of the ZDI are shown by the black line. (b)-(d) Same as (a), but for the relations with (b) the meridional wind anomaly averaged over the Norwegian Sea (green box in Fig. 3c), and geopotential height anomalies averaged over (c) GB and (d) ST regions (grey boxes in Fig. 3b). Weekly averages within a 30-day period after SSW events are marked by red triangles. Only SSWs with a strong Barents Sea response are shown. Linear regression lines are computed for climatology (black) and SSW events (red). The corresponding R^2 coefficients are indicated in each panel. For comparison, the correlation coefficient for weekly averages excluding the 30-day periods after SSW events is indicated (blue). All anomalies are computed with respect to the daily climatology.

are generally associated with cold surface weather over Europe. It however remains unclear how often a strong projection of dominant geopotential height anomalies on the MCAO index occurs in climatology, and how it relates to the large-scale dipole pattern found after SSW events with a strong Barents Sea MCAO response.

For this purpose, we examine composites of the geopotential height and meridional wind anomalies for periods of increased MCAO index over the Barents Sea in climatology using daily means. Strong Barents Sea MCAOs are identified using the criterion of M≥4K (Fig. 5a). Such periods of strong Barents Sea MCAOs are found to be associated with a dipole pattern of geopotential height anomaly, with a high-pressure anomaly south of Greenland and a low-pressure anomaly over Northern Europe, reminiscent of the Atlantic Ridge regime (Fig. 5b). In the upper troposphere, the meridional wind exhibits a negative anomaly north of Scandinavia and the Nordic seas, indicating strong northerly winds over this region (Fig. 5c). It appears that this large-scale atmospheric circulation pattern provides favorable conditions for MCAOs over the Barents Sea, in agreement with previous studies (Kolstad et al., 2009). For the climatological conditions, however, the maximum of the meridional wind

anomalies is found further eastward (Fig. 5c) as compared to the position of the maximum meridional winds after SSW events with a strong Barents Sea response (Fig. 3c). Cyclone frequency in periods of enhanced MCAOs in the Barents Sea indicates an increase in storminess over the Barents Sea (Fig. 3d) relative to DJFM climatology (shown by the black contours), and a decrease over Greenland and the Irminger Sea.

185 As discussed in subsection 3.2, the ZDI index is found to be positively correlated to the MCAO index in climatology (Fig. 4a). In fact, a positive ZDI occurs nearly 50% of the time in DJFM, indicating the likelihood of a dipole pattern occurrence (as shown in Fig. 5b), while an opposite dipole pattern is likely to occur for a combination of different circulation patterns. Consistent with that, a stronger northerly flow over the Norwegian Sea (negative values in Fig. 4b) is found to be correlated with a larger MCAO index over the Barents Sea.

190 An analysis of the relation to the GB and ST geopotential height anomalies in climatology reveals that most of the variance found for the ZDI index (Fig. 5a) can be attributed to the ST index (Fig. 4d), while the relation to the GB index exhibits a much larger variability (Fig. 4c).

Thus, linearly regressing the geopotential height and meridional wind indices on the MCAO frequency demonstrates a similar dependence as that found for the MCAO index, with a positive relation between the ZDI and Z'_{GB} indices, and the
195 MCAO frequency, and a negative relation for the meridional wind anomaly and the Z'_{ST} index.

3.3.1 Relative importance of Greenland Blocking and Scandinavian Trough weather patterns for MCAOs in the Barents Sea

A large-scale dipole pattern is found to dominate the North Atlantic and Eurasian sector in periods of strong MCAOs in the Barents Sea. This pattern consists of nearly equally-strong and opposite pressure anomalies over Greenland and Scandinavia.
200 Fig. 6 shows the MCAO index for periods of GB and ST geopotential height anomalies separately. These periods are defined as days for which the 500-hPa geopotential height anomaly averaged over the GB and ST boxes is positive (i.e., Greenland blocking) or negative (i.e., Scandinavian Trough), respectively. Results show that for both GB and ST the circulation over the Barents Sea is cyclonic (Fig. 6a,b) and there is an increase in the MCAO index over the Barents Sea (Fig. 6c and Fig. 6d, respectively). Interestingly, only the GB pattern is accompanied by a reduced frequency of MCAOs in the Labrador Sea. These
205 differences are clearly related to the differences in storminess (Fig. 6e,f). Indeed, periods of negative ST are associated with increased storminess over Scandinavia and the southern Barents Sea, whereas periods of GB exhibit a strong reduction in cyclone frequency over the Nordic Seas centered over the Irminger Sea.

The dependency of the MCAO index in the Barents Sea on the GB and ST indices is shown in Fig. 7. Strong MCAOs (represented by yellow marker color) tend to be associated with a negative ST index for either a negative or a positive GB
210 index. The most intense MCAOs, however, are found for negative ST index and positive GB index, emphasizing the importance of this particular combination for the occurrence of MCAOs in the Barents Sea (this pattern is consistent with a positive ZDI index).
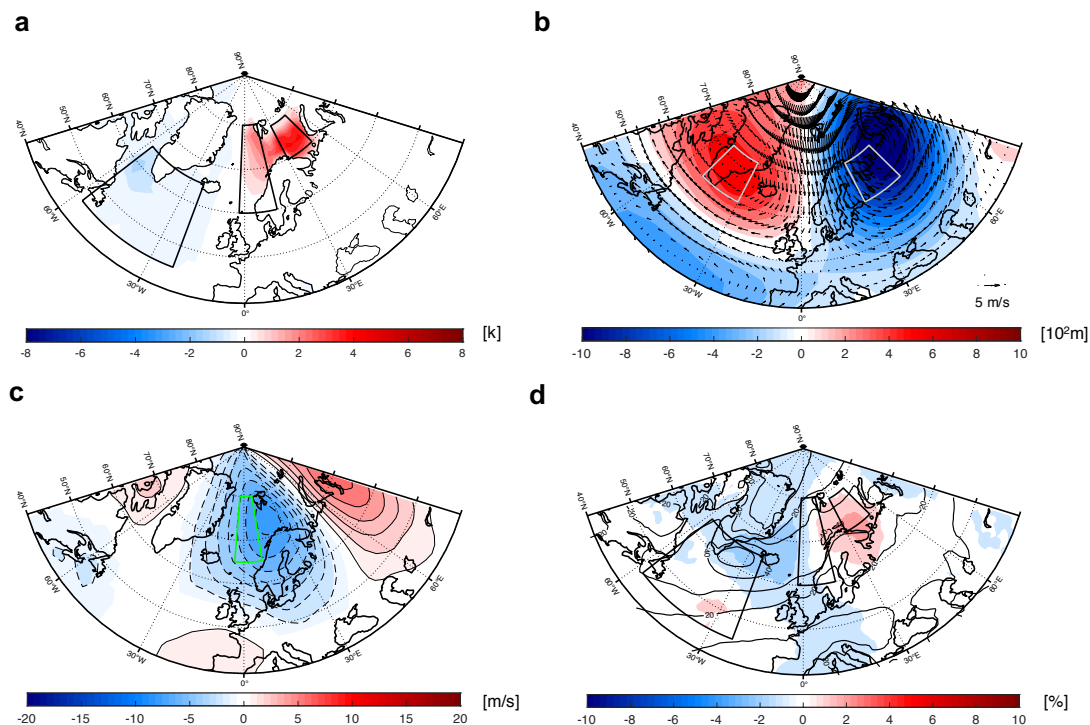
Figure 5. Regional flow patterns during periods of strong Barents Sea MCAO index (M≥4K) in DJFM. Composites of daily averages of (a) MCAO index anomaly (color shading, in K), (b) geopotential height anomaly at 500 hPa (shading, in 10^2m), and (c) meridional wind anomaly at 300 hPa (shading, in m s^{-1}) averaged over periods of strong MCAOs in the Barents Sea (M≥4K) as in (a). Wind anomalies at 300 hPa are indicated in panel (b) (arrows, in m s^{-1}). (d) Cyclone frequency anomaly (shading) for strong MCAOs in the Barents Sea as in (a). Winter (DJFM) climatology of cyclone frequency is shown by black contours (from 10%, in intervals of 10%). Only statistically significant values above the 95% level are shown (based on a two-sided Student's *t test)*.

4 Conclusions

This study focuses on the influence of the stratosphere on the occurrence of marine cold air outbreaks in the Barents Sea and
215   their connection to the large-scale circulation patterns over the North Atlantic and Europe. Particularly, we investigate how the
frequency and the magnitude of such MCAOs in the Barents Sea are affected by the large-scale conditions after the onset of
extreme events in the stratosphere, known as SSW events.

    After two thirds of SSW events, significant changes in the large-scale atmospheric circulation occur (e.g., Karpechko et al.,
2017; Afargan-Gerstman and Domeisen, 2020). We show that these changes are often followed by a more frequent occurrence
220   of MCAOs in the Barents Sea in the ERA-Interim reanalysis. Analyzing the regional atmospheric conditions following SSW
events with enhanced Barents Sea response suggests that a higher 500 hPa geopotential height anomaly over Greenland and
a lower geopotential height anomaly over Scandinavia, accompanied by increased northerly winds over the Norwegian Sea
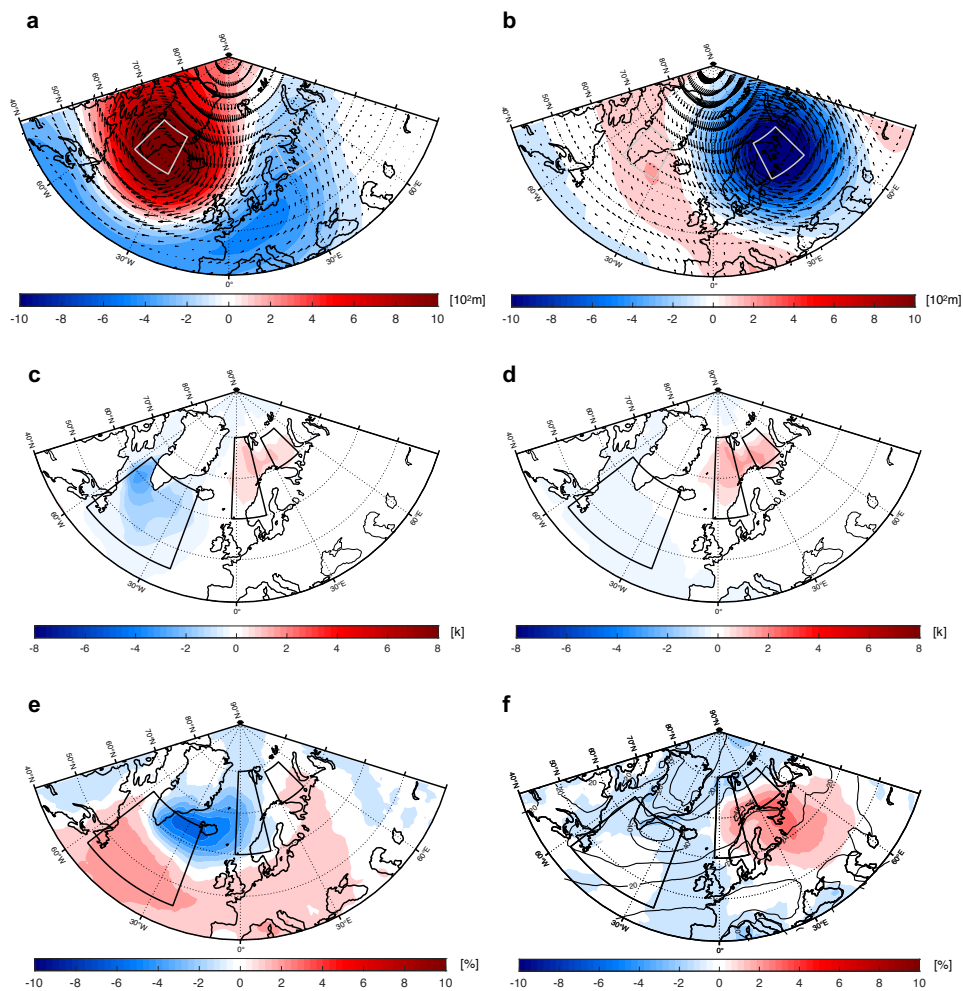
Figure 6. Regional patterns for the Greenland Blocking (GB) and Scandinavian Trough (ST) composites in DJFM. (a,b) Geopotential height anomaly at 500 hPa (color shading, in 10^2 m) and wind at the same pressure level (arrows, in m s^{-1}), (c,d) MCAO index anomaly (color shading, in K), and (e,f) mean cyclone frequency (shading, in %) for days with (left column) positive 500-hPa geopotential height anomaly averaged over the GB box, and (right column) negative anomaly averaged over the ST box, respectively. Black contours in panels (e,f) show the DJFM climatology of cyclone frequency (from 10%, in intervals of 10%). Only statistically significant values above the 95% level are shown (based on a two-sided Student's *t test).*
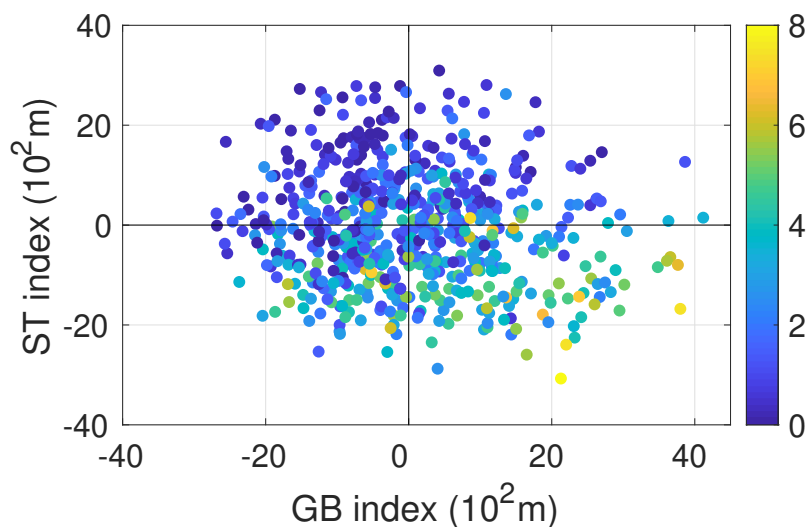
Figure 7. Scatter plot of weekly means of 500-hPa geopotential height anomalies (in 10^2 m) averaged over the Greenland Blocking (GB) and Scandinavian Trough (ST) boxes (westernmost and easternmost gray boxes in Fig. 4b, respectively) during DJFM. As in Fig. 4, all anomalies are computed with respect to the daily climatology and averaged weekly. Marker color indicates the mean MCAO index (K) averaged over the Barents Sea.

and increased storminess over the Barents Sea, are strong indicators for more frequent MCAOs in the Barents Sea. After SSW events, this large-scale atmospheric circulation pattern, represented by a positive zonal dipole index, accounts for 44% of the
225 MCAO variance in the Barents Sea, compared to 11% of the variance in winters without SSW events.

Understanding the connection between MCAOs in the Arctic and the stratosphere provides a key for improved predictive skill of cold air outbreaks on subseasonal to seasonal time scales. An example for such implication for sub-seasonal climate forecasts of MCAOs can be found in Polkova et al. (2019), who found a high prediction skill for MCAOs over the Barents Sea, Norwegian Sea and the Labrador Sea using the seasonal prediction system based on the Earth System Model from the
230 Max-Planck Institute for Meteorology (MPI-ESM). According to their analysis, MCAOs can be predicted about 2.5 weeks ahead, starting from November initial conditions. Our results show that subseasonal predictors, such as the stratosphere, lead to an increased likelihood of the favorable conditions for MCAOs in the Barents Sea (Fig. 4). This connection can potentially be exploited for improving subseasonal predictions.

More generally, we find that the most intense MCAOs in winter occur for a combination of dominant low pressure anomalies
235 over Scandinavia (i.e., a negative ST index) and high pressure anomalies over Greenland (i.e., a positive GB index). This suggests that a specific combination of large-scale circulation patterns is responsible for the favorable conditions for MCAOs in the Barents Sea (see section 3.3.1). This pattern is also consistent with a dipole pattern anomaly (i.e., a positive ZDI index) over the Euro-Atlantic sector, and may also indicate the pathway of cold air masses during MCAO formation. MCAO air masses over the Barents Sea tend to originate in the high or Siberian Arctic, with dominant pathways of cold air masses from
240 Siberia across Novaja Zemlja and the northern sea ice edge into the Barents Sea (Papritz and Spengler, 2017). The northern

pathway is largely captured by a positive ZDI index and is consistent with a low pressure anomaly over north-eastern Europe, bringing cold air masses southward over the Norwegian Sea. A negative ZDI index, on the other hand, may be linked to a dominant blocking pattern over the Barents and Kara Seas, possibly related to the eastern pathway for MCAOs in the Barents Sea.

245   We conclude that understanding the connection between stratospheric forcing and the occurrence of MCAOs in the Arctic can highlight the key ingredients of MCAO formation in these regions, which can potentially lead to improved prediction skill on subseasonal to seasonal time scales. We find that a weakening of the polar vortex associated with SSW events leads to a reduction in MCAO frequency in the Labrador and the Irminger Seas, and an increase over the Barents Sea.

It is worth noting that the reduction in MCAO frequency in the Labrador Sea after SSW events has received little attention
250   in previous studies, despite their importance for dense water formation. A suppression of MCAOs in the Labrador Sea, as often occurs after SSW events, may therefore have a substantial impact on the North Atlantic overturning circulation.

An additional factor that affects the occurrence of MCAOs is sea ice cover in the Barents Sea (e.g., Ruggieri et al., 2016). In a warming climate, the diminishing sea ice cover over the Barents Sea can potentially shift MCAO occurrence in this region, by exposing more of the ocean surface to interaction with the atmosphere. Such changes are also likely to be affected by the
255   availability of cold air masses in the Arctic (e.g., Papritz et al., 2019). Further work is however required for understanding the sea ice impact and feedback on MCAO formation.

Author contributions. H.A-G. and D.D. initiated and led the study. I.P., P.R. and M.K. contributed ideas on the early stage of the study. H.A-G. performed the analysis and created all figures and tables. L.P. provided the cyclone frequency datasets and contributed to the interpretation of the results. H.A-G. wrote the manuscript with contributions from all authors.

260   *Competing interests.* The authors declare no competing interests.

Acknowledgements. Funding by the European Union's Horizon 2020 research and innovation programme has been received by H.A-G., I.P., P.R., M.K., P.A., J.B., and D.D. for the Blue Action project under Grant Agreement 727852. ERA-Interim reanalysis has been obtained from the ECMWF server (https://apps.ecmwf.int/datasets/data/). Funding to D.D. by the Swiss National Science Foundation through grant No. PP00P2_170523 is gratefully acknowledged.

References

Afargan-Gerstman, H. and Domeisen, D. I. V.: Pacific modulation of the North Atlantic storm track response to sudden stratospheric warming events, Geophysical Research Letters, p. e2019GL085007, 2020.

Baldwin, M. P. and Dunkerton, T. J.: Stratospheric harbingers of anomalous weather regimes, Science, 294, 581–584, 2001.

Beerli, R. and Grams, C. M.: Stratospheric modulation of the large-scale circulation in the Atlantic–European region and its implications for surface weather events, Quarterly Journal of the Royal Meteorological Society, 145, 3732–3750, 2019.

Buckley, M. W. and Marshall, J.: Observations, inferences, and mechanisms of Atlantic Meridional Overturning Circulation variability: A review, Rev. Geophys., 54, 5–63, https://doi.org/10.1002/2015RG000493, 2016.

Butler, A. H., Sjoberg, J. P., Seidel, D. J., and Rosenlof, K. H.: A sudden stratospheric warming compendium., Earth System Science Data, 9, 2017.

Charlton, A. J. and Polvani, L. M.: A new look at stratospheric sudden warmings. Part I: Climatology and modeling benchmarks, Journal of Climate, 20, 449–469, 2007.

Cohen, J., Screen, J. A., Furtado, J. C., Barlow, M., Whittleston, D., Coumou, D., Francis, J., Dethloff, K., Entekhabi, D., Overland, J., and Jones, J.: Recent Arctic amplification and extreme mid-latitude weather, Nat. Geosci., 7, 627–637, https://doi.org/10.1038/ngeo2234, 2014.

Dee, D. P., Uppala, S. M., Simmons, A., Berrisford, P., Poli, P., Kobayashi, S., Andrae, U., Balmaseda, M., Balsamo, G., Bauer, d. P., et al.: The ERA-Interim reanalysis: Configuration and performance of the data assimilation system, Quarterly Journal of the royal meteorological society, 137, 553–597, 2011.

Domeisen, D. I. V.: Estimating the Frequency of Sudden Stratospheric Warming Events from Surface Observations of the North Atlantic Oscillation, Journal of Geophysical Research: Atmospheres, 124, 3180–3194, 2019.

Domeisen, D. I. V., Butler, A. H., Charlton-Perez, A. J., Ayarzagüena, B., Baldwin, M. P., Sigouin, E. D., Furtado, J. C., Garfinkel, C. I., Hitchcock, P., Karpechko, A. Y., Kim, H., Knight, J., Lang, A. L., Lim, E.-P., Marshall, A., Roff, G., Schwartz, C., Simpson, I. R., Son, S.-W., and Taguchi, M.: The role of the stratosphere in subseasonal to seasonal prediction: 2. Predictability arising from stratosphere - troposphere coupling, Journal of Geophysical Research-Atmospheres, https://doi.org/10.1029/2019JD030923, 2019.

Domeisen, D. I. V., Grams, C. M., and Papritz, L.: The role of North Atlantic-European weather regimes in the surface impact of sudden stratospheric warming events, Weather Clim. Dynam. Discuss., https://doi.org/doi:10.5194/wcd-2019-16, 2020.

Isachsen, P., Drivdal, M., Eastwood, S., Gusdal, Y., Noer, G., and Saetra, Ø.: Observations of the ocean response to cold air outbreaks and polar lows over the Nordic Seas, Geophysical Research Letters, 40, 3667–3671, 2013.

Jahnke-Bornemann, A. and Brümmer, B.: The Iceland-Lofotes pressure difference: different states of the North Atlantic low-pressure zone, Tellus A, 61, 466–475, https://doi.org/10.1111/j.1600-0870.2009.00401.x, 2009.

Karpechko, A. Y., Hitchcock, P., Peters, D. H., and Schneidereit, A.: Predictability of downward propagation of major sudden stratospheric warmings, Quarterly Journal of the Royal Meteorological Society, 143, 1459–1470, 2017.

Kidston, J., Scaife, A. A., Hardiman, S. C., Mitchell, D. M., Butchart, N., Baldwin, M. P., and Gray, L. J.: Stratospheric influence on tropospheric jet streams, storm tracks and surface weather, Nature Geoscience, 8, 433, 2015.

Kolstad, E. W.: A global climatology of favourable conditions for polar lows, Quarterly Journal of the Royal Meteorological Society, 137, 1749–1761, 2011.

Kolstad, E. W.: Higher ocean wind speeds during marine cold air outbreaks, Quarterly Journal of the Royal Meteorological Society, 143, 2084–2092, 2017.

Kolstad, E. W. and Bracegirdle, T. J.: Marine cold-air outbreaks in the future: an assessment of IPCC AR4 model results for the Northern Hemisphere, Clim. Dyn., 30, 871–885, https://doi.org/10.1007/s00382-007-0331-0, 2008.

305 Kolstad, E. W., Bracegirdle, T. J., and Seierstad, I. A.: Marine cold-air outbreaks in the North Atlantic: temporal distribution and associations with large-scale atmospheric circulation, Climate dynamics, 33, 187–197, 2009.

Kolstad, E. W., Breiteig, T., and Scaife, A. A.: The association between stratospheric weak polar vortex events and cold air outbreaks in the Northern Hemisphere, Quarterly Journal of the Royal Meteorological Society, 136, 886–893, 2010.

Kretschmer, M., Coumou, D., Agel, L., Barlow, M., Tziperman, E., and Cohen, J.: More-persistent weak stratospheric polar vortex states

310   linked to cold extremes, Bulletin of the American Meteorological Society, 99, 49–60, 2018.

Limpasuvan, V., Thompson, D. W., and Hartmann, D. L.: The life cycle of the Northern Hemisphere sudden stratospheric warmings, Journal of Climate, 17, 2584–2596, 2004.

Mallet, P.-E., Claud, C., Cassou, C., Noer, G., and Kodera, K.: Polar lows over the Nordic and Labrador Seas: Synoptic circulation patterns and associations with North Atlantic-Europe wintertime weather regimes, Journal of Geophysical Research: Atmospheres, 118, 2455–

315   2472, 2013.

Mansfield, D.: Polar lows: The development of baroclinic disturbances in cold air outbreaks, Quarterly Journal of the Royal Meteorological Society, 100, 541–554, 1974.

Papritz, L. and Grams, C. M.: Linking low-frequency large-scale circulation patterns to cold air outbreak formation in the northeastern North Atlantic, Geophysical Research Letters, 45, 2542–2553, 2018.

320 Papritz, L. and Spengler, T.: A Lagrangian climatology of wintertime cold air outbreaks in the Irminger and Nordic Seas and their role in shaping air–sea heat fluxes, Journal of Climate, 30, 2717–2737, 2017.

Papritz, L., Pfahl, S., Sodemann, H., and Wernli, H.: A climatology of cold air outbreaks and their impact on air–sea heat fluxes in the high-latitude South Pacific, Journal of Climate, 28, 342–364, 2015.

Papritz, L., Rouges, E., Aemisegger, F., and Wernli, H.: On the thermodynamic pre-conditioning of Arctic air masses and the role of

325   tropopause polar vortices for cold air outbreaks from Fram Strait, Journal of Geophysical Research: Atmospheres, 2019.

Polkova, I., Afargan-Gerstman, H., Domeisen, D., Ruggieri, P., Athanasiadis, P., King, M., and Baehr, J.: Marine Cold Air Outbreaks: Prediction Skill and Preconditions, Proceedings of the Ninth International Workshop on Climate Informatics: CI 2019. NCAR Technical Note NCAR/TN-561+PROC, pp. 25–31, https://doi.org/10.5065/y82j-f154, 2019.

Radovan, A., Crewell, S., Moster Knudsen, E., and Rinke, A.: Environmental conditions for polar low formation and development over the

330   Nordic Seas: study of January cases based on the Arctic System Reanalysis, Tellus A: Dynamic Meteorology and Oceanography, 71, 1–16, 2019.

Rasmussen, E. A., Turner, J., and Thorpe, A.: Polar lows: Mesoscale weather systems in the polar regions, Quarterly Journal of the Royal Meteorological Society, 130, 371–372, 2004.

Ruggieri, P., Buizza, R., and Visconti, G.: On the link between Barents-Kara sea ice variability and European blocking, J. Geophys. Res.

335   Atmos., 121, 5664–5679, https://doi.org/10.1002/2015JD024021, 2016.

Scaife, A., Karpechko, A. Y., Baldwin, M., Brookshaw, A., Butler, A., Eade, R., Gordon, M., MacLachlan, C., Martin, N., Dunstone, N., et al.: Seasonal winter forecasts and the stratosphere, Atmospheric Science Letters, 17, 51–56, 2016.

Sigmond, M., Scinocca, J., Kharin, V., and Shepherd, T.: Enhanced seasonal forecast skill following stratospheric sudden warmings, Nature
Geoscience, 6, 98, 2013.

340 Thompson, D. W., Baldwin, M. P., and Wallace, J. M.: Stratospheric connection to Northern Hemisphere wintertime weather: Implications
for prediction, Journal of Climate, 15, 1421–1428, 2002.

Wernli, H. and Schwierz, C.: Surface cyclones in the ERA-40 dataset (1958–2001). Part I: Novel identification method and global climatol-
ogy, Journal of the atmospheric sciences, 63, 2486–2507, 2006.